Acta Cryst. (1984). B40, 126–132

New Series of Superstructures Based on a Clinopyroxene. II. The Structure of the Sc Series of Enstatite-IV, $[Mg_{\sim(x-7\cdot5)/3}Sc_{\sim3}][Mg_{2/3}Si_{(x-4)/3}]O_x$, with $x = 100$, 112 or 124

BY YOSHIO TAKÉUCHI, HIROSHI MORI AND YASUHIRO KUDOH

Mineralogical Institute, Faculty of Science, University of Tokyo, Hongo, Tokyo 113, *Japan*

AND JUN ITO*

James Franck Institute, University of Chicago, Chicago, IL 60637, *USA*

(*Received* 14 *October* 1983; *accepted* 16 *November* 1983)

Abstract

A new chemical series which is similar to 'enstatite-IV' (En-IV) but free from Li has been discovered and called the 'Sc series of enstatite-IV'. Like the crystals of En-IV, those of the new series, which has been denoted EnIV', crystallize in three structure types: En-IV-10, En-IV-9, or En-IV-8, depending upon the Sc content in the crystals. Those having these structure types have been denoted EnIV'-10, EnIV'-9 and EnIV'-8, respectively. Structure analyses revealed that, unlike En-IV, they characteristically contain Mg at the T site with an occupancy of at most 33·3%, giving structure formulae which may be well approximated by the general form $[Mg_{\sim(x-7\cdot5)/3}Sc_{\sim3}][Mg_{2/3}Si_{(x-4)/3}]O_x$. EnIV'-10: $a = 9\cdot424\,(2)$, $b = 8\cdot738\,(2)$, $c = 27\cdot021\,(8)$ Å, $\beta = 93\cdot24\,(2)°$, $P2/a$, $Z = 1$, $x = 124$; EnIV'-9: $a = 9\cdot424\,(1)$, $b = 8\cdot740\,(1)$, $c = 48\cdot808\,(6)$ Å, $\beta = 92\cdot38\,(1)°$, $I2/a$, $Z = 2$, $x = 112$; EnIV'-8: $a = 9\cdot434\,(1)$, $b = 8\cdot731\,(1)$, $c = 21\cdot791\,(4)$ Å, $\beta = 91\cdot30\,(1)°$, $P2/a$, $Z = 1$, $x = 100$.] Their structural data, such as bond lengths and bond angles, are closely similar to those of the corresponding En-IV structures. Evidence has been presented for the existence of further complex structures in this series.

Introduction

At an early stage of the structural study on En-IV (see part I, Takéuchi, Kudoh & Ito, 1984), there was an argument concerning the Li content of the material. This argument eventually led us to synthesize another new chemical series of magnesium scandium silicates which are isotypic with En-IV but free from Li. The study on the structures of this series has revealed further detailed features of the En-IV structure type, particularly those of the tetrahedra, denoted T, that occur at the boundaries of the CPX slabs. The present paper describes and discusses the results of our study on this new chemical series which we call the 'Sc series of enstatite-IV' and denote EnIV'. Symbols such as CPX, **M1**, and **M2** are explained in part I.

Experimental

Using MgO, Sc_2O_3, and H_2SiO_3 as starting materials, we synthesized the crystals of the Sc series of En-IV similarly to the method for En-IV (see part I). Crystals obtained were transparent and platy parallel to (001), similar to those of En-IV. They exhibited, however, pronounced parting parallel to (100) which was not significant for the En-IV crystals. By means of the X-ray precession method, they were found to be isotypic with En-IV. If the starting mixtures contained about 5 mol % Sc_2O_3, the resulting crystals had the structure type of En-IV-10, and if about 7 mol % the products were mostly of the En-IV-8 type. Crystals having the structure type En-IV-9 were obtained from starting mixtures containing Sc_2O_3 in amounts between 5 and 7 mol %. These three kinds of new crystalline phases having the structure type of En-IV-N will be denoted EnIV'-N, where $N = 8$, 9, or 10. From the synthetic samples having each structure type, a piece of crystal was selected and used for the present structural study. Each crystal selected is denoted in what follows by the same symbol as that used for its structure type.

The cell dimensions of the crystals (Table 1) were obtained by the least-squares procedure applied to $\sin 2\theta$ values of 15 reflections which were measured with a single-crystal Syntex $P2_1$ diffractometer using graphite-monochromated Cu $K\alpha$ radiation ($\lambda = 1\cdot54178$ Å). These cell dimensions should be compared with those of En-IV given in part I.

The ω–2θ scan technique was used to measure reflection intensities; Table 2 lists the intensity-study data. Reflection intensities were corrected for Lorentz and polarization factors as well as for absorption. For EnIV'-10, EnIV'-9, the latter corrections were made with the computer program *ACACA* (Wuensch

* Deceased 6th June 1978.

0108-7681/84/020126-07$01.50

Table 1. *Crystal data of En*IV′

	EnIV′-10	EnIV′-9	EnIV′-8
Axes set *A*			
a (Å)	9·424 (2)	9·424 (1)	9·434 (1)
b (Å)	8·738 (2)	8·740 (1)	8·731 (1)
c (Å)	55·380 (16)	50·092 (6)	44·797 (8)
β (°)	103·02 (2)	103·21 (1)	103·44 (1)
V (Å^3)	4443·13	4016·39	3588·80
Space group	*B*2/*a*	*A*2/*a*	*B*2/*a*
Axes set *B*			
a (Å)	9·424 (2)	9·424 (1)	9·434 (1)
b (Å)	8·738 (2)	8·740 (1)	8·731 (1)
c (Å)	27·021 (8)	48·808 (6)	21·791 (4)
β (°)	93·24 (2)	92·38 (1)	91·30 (1)
Space group	*P*2/*a*	*I*2/*a*	*P*2/*a*
CPX subcell			
a (Å)	9·791	9·789	9·788
b (Å)	8·738	8·756	8·740
c (Å)	5·538	5·566	5·600
β (°)	110·41	110·40	110·37

Table 2. *Intensity-study data*

	EnIV′-10	EnIV′-9	EnIV′-8
Crystal size (mm)	0·32×0·19 ×0·09	0·33×0·25 ×0·12	0·25 (diameter)
μ (cm^{-1}) for Cu $K\alpha$	112·0	115·7	116·1
Number of reflections ($2\theta < 130°$)			
measured	4093	3792	3344
used	2755	2757	2803
R (%) isotropic	7·34	5·72	4·52
R (%) anisotropic	6·77	4·58	3·97

Table 3. *Chemical composition* (wt%)

	EnIV′-10	EnIV′-9	EnIV′-8
SiO_2	58·66	57·26	56·39
MgO	38·24	36·84	37·61
Sc_2O_3	4·28	5·07	5·54
Total	101·18	99·17	99·54

& Prewitt, 1965). We employed a spherical absorption correction for EnIV′-8, because the crystal was ground to the shape of a sphere to a good approximation.

The crystals used for the measurements of reflection intensities were then subjected to chemical analysis. The listing of the chemical composition in Table 3 for each crystal is an average of the results of electron-microprobe analyses at five sampling points of the crystal (analyst: H. Mori). We may then express the chemical formulae in the following way taking into account the results of the structure analyses which are described below:

EnIV′-10

$$(Mg_{39\cdot20}Sc_{2\cdot56}\square_{0\cdot24})[(Mg_{0\cdot08}Si_{0\cdot44}\square_{1\cdot48})Si_{40}]O_{124} \quad (1)$$

EnIV′-9

$$(Mg_{34\cdot80}Sc_{2\cdot98}\square_{0\cdot22})[(Mg_{0\cdot32}Si_{0\cdot24}\square_{1\cdot44})Si_{36}]O_{112} \quad (2)$$

EnIV′-8

$$(Mg_{31\cdot24}Sc_{2\cdot76})[(Mg_{0\cdot60}Si_{0\cdot04}\square_{1\cdot36})Si_{32}]O_{100}. \quad (3)$$

Structure analysis

The structures of En-IV-10, En-IV-9, and En-IV-8 (see part I) provided initial sets of atomic parameters for the structure analyses of the present crystals having the corresponding structure types. In the *T* site of each structure, however, the amount of Si located exceeded the number of Si positions in the CPX slab. The least-squares refinement of the structure was initiated by refining the atomic coordinates and isotropic temperature factors of each structure with the use of *LINUS* (Coppens & Hamilton, 1970). After the refinement converged, a preliminary occupancy refinement was executed without a constraint on chemical composition; the total of the resulting number of Mg per cell tended to be lower than that obtained by the chemical analysis.

We then located Mg at the *T* site in addition to the excess Si atoms and refined the occupancy parameter of the Mg atom. In each case, the refinement converged with the Mg occupancy at the same value regardless of the values initially assumed. The significance of the resulting contents at the *T* site was confirmed by difference Fourier syntheses. Finally, the structure was refined by the anisotropic least-squares procedure with the occupancy at *T* being fixed and with those at the cation sites, other than Si, being constrained by chemical composition. The final values of *R* are listed in Table 2. For structure factor calculation we used fully ionized form factors from *International Tables for X-ray Crystallography* (1962). Unit weight was used for least-squares calculations. In the final refinement cycles for the three structures, the ratios of average and maximum shifts to error are in the ranges 0·05 ~ 0·15 and 0·40 ~ 0·95, respectively. In Tables 4, 5 and 6 we give the final atomic coordinates, referred to the *B* set of axes (Table 1), and isotropic temperature factors for EnIV′-10, EnIV′-9, and EnIV′-8, respectively.*

Discussion

Structural similarity between En-IV *and En*IV′

The crystal structures of the Sc series of En-IV thus obtained are closely similar to the corresponding structures of the En-IV series. As an example, the bond lengths of EnIV′-10 are listed in Table 7, which is to be compared with those for En-IV-10 given in Table 8 of part I. The Sc atoms are mainly distributed over the cation sites which belong to **M1** (Table 8). The Sc contents of the cation sites which belong to **M2** are negligible except those at the sites closest to

* Lists of structure factors, anisotropic temperature factor coefficients and bond lengths (for EnIV′-9 and EnIV′-8) have been deposited with the British Library Lending Division as Supplementary Publication No. SUP 38999 (66 pp.). Copies may be obtained through The Executive Secretary, International Union of Crystallography, 5 Abbey Square, Chester CH1 2HU, England.

Table 4. *Atomic parameters of En*IV′-10 (*fractional atomic coordinates are multiplied by* 10^4)

	x	y	z	B (Å^2)		x	y	z	B (Å^2)
M(1)	2500	1498 (6)	0	0·58 (7)	O(4)	5609 (8)	2351 (9)	1004 (3)	0·6 (1)
M(2)	2106 (4)	3505 (4)	990 (1)	0·60 (5)	O(5)	3132 (8)	1551 (9)	1401 (3)	0·5 (1)
M(3)	1698 (4)	1485 (4)	1979 (1)	0·59 (5)	O(6)	5660 (8)	16 (9)	1531 (3)	0·6 (1)
M(4)	1241 (4)	3521 (4)	2967 (1)	0·54 (5)	O(7)	5222 (8)	2735 (9)	1954 (3)	0·5 (1)
M(5)	720 (4)	1505 (4)	3945 (1)	0·62 (6)	O(8)	2721 (8)	3432 (9)	2378 (3)	0·5 (1)
M(6)	−792 (4)	3399 (4)	4919 (1)	1·00 (6)	O(9)	5235 (8)	4790 (9)	2510 (3)	0·5 (1)
M(7)	7500	4879 (7)	0	0·67 (7)	O(10)	4819 (8)	2207 (9)	2896 (3)	0·4 (1)
M(8)	7096 (4)	119 (5)	987 (2)	0·67 (5)	O(11)	2289 (8)	1614 (10)	3342 (3)	0·6 (1)
M(9)	6675 (4)	4890 (5)	1973 (1)	0·66 (5)	O(12)	4791 (8)	46 (9)	3489 (3)	0·6 (1)
M(10)	6269 (4)	131 (5)	2968 (1)	0·71 (5)	O(13)	4409 (8)	2900 (9)	3826 (3)	0·6 (1)
M(11)	5881 (4)	4896 (5)	3983 (1)	0·91 (6)	O(14)	1880 (8)	3236 (10)	4284 (3)	1·2 (1)
M(12)	5304 (5)	−16 (8)	4970 (3)	0·6 (1)	O(15)	4411 (8)	4785 (9)	4517 (3)	1·0 (1)
Si(1)	5230 (3)	3403 (3)	512 (1)	0·32 (4)	O(16)	4164 (8)	2002 (10)	4750 (3)	1·0 (1)
Si(2)	4842 (3)	1602 (3)	1482 (1)	0·29 (4)	O(17)	8548 (8)	22 (10)	451 (3)	0·8 (1)
Si(3)	4432 (3)	3401 (7)	2444 (1)	0·33 (4)	O(18)	11092 (8)	1532 (9)	566 (3)	0·6 (1)
Si(4)	4007 (3)	1636 (4)	3397 (1)	0·43 (4)	O(19)	8633 (9)	2546 (10)	893 (3)	0·9 (1)
Si(5)	3597 (3)	3222 (4)	4353 (1)	0·87 (4)	O(20)	8129 (8)	4947 (10)	1448 (3)	0·8 (1)
Si(6)	9386 (3)	1601 (3)	457 (1)	0·34 (4)	O(21)	10680 (8)	3461 (9)	1548 (3)	0·6 (1)
Si(7)	8987 (3)	3386 (4)	1425 (1)	0·34 (4)	O(22)	8260 (9)	2299 (10)	1829 (3)	0·9 (1)
Si(8)	8573 (3)	1624 (4)	2387 (1)	0·42 (4)	O(23)	7690 (8)	91 (10)	2445 (3)	0·8 (1)
Si(9)	8077 (3)	3332 (4)	3334 (1)	0·59 (4)	O(24)	10255 (8)	1542 (10)	2525 (3)	0·6 (1)
Si(10)	7455 (3)	1648 (4)	4246 (1)	0·89 (4)	O(25)	7873 (8)	2861 (9)	2748 (3)	0·9 (1)
T	2500	1141 (22)	5000	0·4 (2)	O(26)	7178 (8)	4827 (10)	3422 (3)	0·8 (1)
O(1)	5989 (8)	2564 (9)	52 (3)	0·8 (1)	O(27)	9749 (8)	3431 (9)	3513 (3)	0·6 (1)
O(2)	3522 (8)	3463 (9)	420 (3)	0·6 (1)	O(28)	7380 (8)	1891 (9)	3631 (3)	0·8 (1)
O(3)	6055 (8)	4988 (10)	541 (3)	0·7 (1)	O(29)	6600 (9)	175 (10)	4410 (3)	1·4 (1)
					O(30)	9097 (8)	1509 (9)	4459 (3)	1·1 (1)
					O(31)	6953 (8)	3233 (10)	4501 (3)	1·3 (1)

Table 5. *Atomic parameters of En*IV′-9 (*fractional atomic coordinates are multiplied by* 10^4)

	x	y	z	B (Å^2)		x	y	z	B (Å^2)
M(1)	2278 (2)	1496 (3)	2775 (1)	0·61 (4)	O(4)	5344 (4)	2280 (5)	3317 (1)	0·58 (7)
M(2)	1826 (2)	3513 (3)	3325 (1)	0·58 (4)	O(5)	2824 (4)	1565 (5)	3547 (1)	0·52 (7)
M(3)	1326 (2)	1480 (3)	3873 (1)	0·53 (4)	O(6)	5339 (4)	5 (5)	3619 (1)	0·62 (7)
M(4)	754 (3)	3492 (3)	4415 (1)	0·68 (5)	O(7)	4902 (4)	2793 (5)	3837 (1)	0·51 (7)
M(5)	−780 (2)	1602 (3)	4956 (1)	0·71 (4)	O(8)	2346 (4)	3393 (5)	4080 (1)	0·54 (7)
M(6)	7273 (2)	4885 (2)	2774 (1)	0·70 (4)	O(9)	4848 (4)	4963 (5)	4162 (1)	0·58 (7)
M(7)	6799 (2)	108 (3)	3321 (1)	0·69 (4)	O(10)	4444 (4)	2097 (5)	4350 (1)	0·57 (7)
M(8)	6346 (2)	4870 (3)	3873 (1)	0·66 (4)	O(11)	1911 (4)	1757 (5)	4602 (1)	0·77 (7)
M(9)	5923 (2)	106 (3)	4437 (1)	0·89 (4)	O(12)	4416 (4)	212 (5)	4733 (1)	0·72 (7)
M(10)	4744 (7)	4970 (10)	5014 (2)	1·0 (1)	O(13)	4172 (4)	3005 (5)	4863 (1)	0·68 (7)
Si(1)	4989 (2)	3393 (2)	3053 (1)	0·41 (3)	O(14)	8745 (4)	4985 (5)	2477 (1)	0·75 (7)
Si(2)	4534 (2)	1596 (2)	3586 (1)	0·38 (3)	O(15)	11280 (4)	3460 (5)	2539 (1)	0·57 (7)
Si(3)	4064 (2)	3367 (2)	4114 (1)	0·44 (3)	O(16)	8805 (5)	2495 (5)	2730 (1)	0·95 (8)
Si(4)	3612 (2)	1785 (2)	4643 (1)	0·63 (3)	O(17)	8281 (4)	47 (5)	3030 (1)	0·72 (7)
Si(5)	9577 (2)	3400 (2)	2484 (1)	0·42 (3)	O(18)	10832 (4)	1543 (5)	3084 (1)	0·52 (7)
Si(6)	9133 (2)	1617 (2)	3020 (1)	0·44 (3)	O(19)	8392 (5)	2689 (5)	3247 (1)	1·04 (8)
Si(7)	8682 (2)	3377 (2)	3553 (1)	0·47 (3)	O(20)	7801 (4)	4918 (5)	3582 (1)	0·64 (7)
Si(8)	8146 (2)	1673 (2)	4079 (1)	0·54 (3)	O(21)	10369 (4)	3453 (5)	3629 (1)	0·56 (7)
Si(9)	7470 (2)	3350 (2)	4582 (1)	0·66 (3)	O(22)	7959 (4)	2136 (5)	3756 (1)	0·86 (8)
T	2500	3902 (24)	5000	0·87 (30)	O(23)	7239 (4)	168 (5)	4126 (1)	0·66 (7)
O(1)	5774 (5)	2611 (5)	2792 (1)	0·75 (7)	O(24)	9811 (4)	1583 (5)	4178 (1)	0·55 (7)
O(2)	3279 (4)	3450 (5)	3006 (1)	0·55 (7)	O(25)	7421 (4)	3121 (5)	4243 (1)	0·67 (7)
O(3)	5812 (4)	4983 (5)	3075 (1)	0·70 (7)	O(26)	6608 (5)	4831 (6)	4673 (1)	1·08 (8)
					O(27)	9121 (4)	3471 (5)	4697 (1)	0·68 (7)
					O(28)	6967 (5)	1757 (5)	4717 (1)	0·78 (7)

Table 6. *Atomic parameters of En*IV′-8 (*fractional atomic coordinates are multiplied by* 10^4)

	x	y	z	B (Å^2)		x	y	z	B (Å^2)
M(1)	2500	1485 (2)	0	0·74 (5)	O(3)	6000 (3)	4980 (4)	674 (1)	0·85 (6)
M(2)	1997 (2)	3518 (2)	1239 (1)	0·79 (3)	O(4)	5499 (3)	2313 (4)	1239 (1)	0·84 (6)
M(3)	1445 (2)	1474 (2)	2474 (1)	0·66 (3)	O(5)	2972 (3)	1560 (4)	1740 (1)	0·70 (6)
M(4)	815 (1)	3494 (2)	3692 (1)	0·76 (3)	O(6)	5477 (3)	10 (4)	1903 (1)	0·72 (6)
M(5)	778 (2)	8396 (2)	5101 (1)	0·99 (4)	O(7)	5009 (3)	2779 (4)	2403 (1)	0·71 (6)
M(6)	7500	4880 (3)	0	0·89 (5)	O(8)	2446 (3)	3392 (4)	2939 (1)	0·68 (6)
M(7)	6972 (2)	114 (2)	1232 (1)	0·87 (3)	O(9)	4933 (3)	4962 (4)	3120 (1)	0·68 (6)
M(8)	6463 (2)	4868 (2)	2471 (1)	0·82 (3)	O(10)	4505 (3)	2099 (4)	3550 (1)	0·76 (6)
M(9)	5984 (2)	108 (2)	3742 (1)	0·99 (3)	O(11)	1963 (3)	1757 (4)	4113 (1)	0·91 (6)
M(10)	4748 (3)	4975 (4)	5030 (2)	0·46 (5)	O(12)	4451 (3)	212 (4)	4403 (1)	0·81 (6)
Si(1)	5178 (1)	3395 (1)	638 (1)	0·54 (2)	O(13)	4190 (4)	3012 (4)	4700 (1)	0·99 (6)
Si(2)	4673 (1)	1596 (1)	1834 (1)	0·50 (2)	O(14)	8485 (3)	39 (4)	571 (1)	0·90 (6)
Si(3)	4154 (1)	3369 (2)	3015 (1)	0·54 (2)	O(15)	11021 (3)	1540 (4)	700 (1)	0·77 (6)
Si(4)	3651 (1)	1784 (2)	4201 (1)	0·77 (3)	O(16)	8564 (4)	2643 (4)	1085 (3)	1·16 (7)
Si(5)	9332 (1)	1614 (1)	565 (1)	0·56 (2)	O(17)	7952 (3)	4922 (4)	1815 (1)	0·85 (6)
Si(6)	8830 (1)	3376 (1)	1762 (1)	0·55 (2)	O(18)	10509 (3)	3457 (4)	1926 (1)	0·79 (6)
Si(7)	8243 (1)	1672 (2)	2944 (1)	0·62 (2)	O(19)	8093 (3)	2152 (4)	2224 (1)	1·03 (6)
Si(8)	7512 (1)	3351 (2)	4066 (1)	0·76 (3)	O(20)	7334 (3)	168 (4)	3043 (1)	0·82 (6)
T	2500	3849 (9)	5000	1·2 (1)	O(21)	9900 (3)	1577 (4)	3163 (1)	0·73 (6)
O(1)	5975 (3)	2546 (4)	73 (2)	1·05 (6)	O(22)	7506 (3)	3122 (4)	3311 (1)	0·91 (6)
O(2)	3481 (3)	3458 (4)	524 (1)	0·72 (6)	O(23)	6644 (4)	4830 (4)	4268 (2)	1·25 (7)
					O(24)	9152 (3)	3486 (4)	4324 (1)	0·94 (6)
					O(25)	6990 (3)	1755 (4)	4369 (2)	1·02 (6)

Table 7. *Bond lengths* (Å) *of the En*IV′-10 *structure*

Estimated errors are ±0·006 Å for *M*–O and Si–O, and ±0·010 Å for *T*–O.

M(1)		*M*(5)		*M*(9)		Si(1)	
–O(17)*a* ×2	2·024	–O(12)*b*	1·999	–O(21)*f*	2·045	–O(3)	1·587
–O(18)*c* ×2	2·080	–O(14)	2·052	–O(8)*i*	2·049	–O(2)	1·617
–O(2) ×2	2·238	–O(29)*b*	2·072	–O(20)	2·025	–O(1)	1·639
Av.	2·114	–O(30)*c*	2·119	–O(9)	2·042	–O(4)	1·642
		–O(27)*c*	2·214	–O(7)	2·324	Av.	1·621
M(2)		–O(11)	2·263	–O(22)	2·756		
–O(3)*f*	2·014	Av.	2·120	Av.	2·207	Si(2)	
–O(20)*f*	2·045					–O(6)	1·587
–O(21)*c*	2·074	*M*(6)		*M*(10)		–O(5)	1·617
–O(2)	2·095	–O(15)*f*	1·934	–O(23)	2·005	–O(7)	1·640
–O(5)	2·224	–O(31)*g*	1·969	–O(11)*j*	2·039	–O(4)	1·649
–O(18)*c*	2·246	–O(30)*c*	2·060	–O(12)	2·038	Av.	1·623
Av.	2·116	–O(16)*g*	2·120	–O(24)*b*	2·088		
		–O(15)*g*	2·299	–O(10)	2·264	Si(3)	
M(3)		–O(31)*c*	2·360	–O(28)	2·545	–O(9)	1·585
–O(6)*b*	2·004	Av.	2·124	Av.	2·163	–O(8)	1·614
–O(23)*b*	2·056					–O(10)	1·640
–O(24)*c*	2·062	*M*(7)		*M*(11)		–O(7)	1·659
–O(5)	2·123	–O(2)*h* ×2	2·049	–O(26)	2·000	Av.	1·625
–O(8)	2·200	–O(3) ×2	2·053	–O(14)*i*	2·025		
–O(21)*c*	2·261	–O(1) ×2	2·481	–O(15)	2·060	Si(4)	
Av.	2·118	Av.	2·194	–O(27)*f*	2·179	–O(12)	1·588
				–O(31)	2·222	–O(11)	1·617
M(4)		*M*(8)		–O(13)	2·246	–O(13)	1·633
–O(9)*f*	1·998	–O(18)*b*	2·041	Av.	2·122	–O(10)	1·665
–O(26)*f*	2·063	–O(5)*j*	2·049			Av.	1·631
–O(27)*c*	2·095	–O(17)	2·051	*M*(12)			
–O(11)	2·156	–O(6)	2·054	–O(16)*k*	1·934	Si(5)	
–O(8)	2·175	–O(4)	2·405	–O(16)	2·119	–O(14)	1·599
–O(24)*c*	2·265	–O(19)	2·588	–O(31)*l*	2·102	–O(16)	1·617
Av.	2·125	Av.	2·198	–O(30)*b*	2·172	–O(15)	1·623
				–O(29)	2·004	–O(13)	1·682
				–O(29)*k*	2·530	Av.	1·630
				Av.	2·144		
				T			
				–O(16) ×2	1·887		
				–O(29)*k* ×2	2·104		
				Av.	1·996		

Si(6)		Si(7)	
–O(17)	1·587	–O(20)	1·588
–O(18)	1·619	–O(21)	1·612
–O(19)	1·633	–O(22)	1·627
–O(1)*d*	1·638	–O(19)	1·627
Av.	1·619	Av.	1·614
Si(8)		Si(9)	
–O(23)	1·588	–O(26)	1·584
–O(24)	1·610	–O(27)	1·624
–O(22)	1·624	–O(25)	1·636
–O(25)	1·628	–O(28)	1·652
Av.	1·613	Av.	1·624
Si(10)			
–O(29)	1·598		
–O(31)	1·626		
–O(30)	1·630		
–O(28)	1·671		
Av.	1·631		

For symmetry code see Table 8 of part I.

the CPX boundaries; namely, *M*(11), *M*(9), and *M*(9) for EnIV′-10, EnIV′-9, and EnIV′-8, respectively. The mode of distribution of the Sc atoms in the CPX slabs is thus basically parallel to those of scandium lithium pyroxenes (Hawthorne & Grundy, 1977; Smyth & Ito, 1977). The Sc contents in EnIV′, however, show the salient feature that they systematically vary from one **M1** octahedron to another as illustrated in Fig. 1(*a*). We observe in this diagram that the Sc contents show the smallest value in the octahedra in the region of the centre of the CPX slab. The contents then gradually increase, particularly in the case of EnIV′-10, as the octahedra approach the slab boundaries. In accordance with such a variation in Sc content, the average bond lengths of individual **M1** octahedra show a similar trend of variation (Fig. 1*b*). The Si–O–Si angles and the isotropic temperature factors of Si likewise vary similarly to those in the En-IV structure series (Fig. 1*c*, *d*). The atoms in the octahedra at the CPX boundaries are also statistically located at centrosymmetric pairs of split positions; the separations of the split pairs are 0·596 Å in the *M*(12) octahedron, 0·504 Å in *M*(10), and 0·495 Å in *M*(10) of the EnIV′-10, EnIV′-9, and EnIV′-8 structures, respectively.

Contents of the T site

The significant difference between En-IV and EnIV′ is in the contents of the *T* site located at the CPX boundaries (Table 9). While the *T* site in the former case characteristically contains Li, that in the latter contains divalent Mg; the EnIV′-8 structure provides a typical example (Table 9). Like En-IV, however, the *T* site in the present case may also contain Si. It is notable that the total of the atomic contents of the *T* site decreases as its Si content increases (Table 9). This situation now confirms that the atomic occupancy of *T* is related to the charge of the cations contained as pointed out in part I. As shown in Fig. 2, which gives a plot of the atomic occupancy in *T* *versus* mean cation charge, $\bar{q}$, the occupancies are close to $\frac{2}{3}$, $\frac{1}{3}$, and 0·75/3 (or $\frac{1}{4}$) for $\bar{q}=1$, 2, and 4, respectively.

Although the mode of variation of the Si contents of the *T* sites from one structure to another in the present case (Table 9) assumes that they may be correlated to the preference of structure type, it would probably not be the case. Instead, by analogy with the En-IV case, we may regard the chemical compositions (1), (2), and (3) as being basically the varieties of those of a chemical series having the following general formula:

$$[Mg_{(x-12)/3}Sc_4][Mg_{2/3}Si_{(x-4)/3}]O_x \qquad (4)$$

with $x=100$, 112, or 124. With respect to the *T* site, the formula thus expressed may be regarded as that for an Mg analogue of En-IV. Available chemical

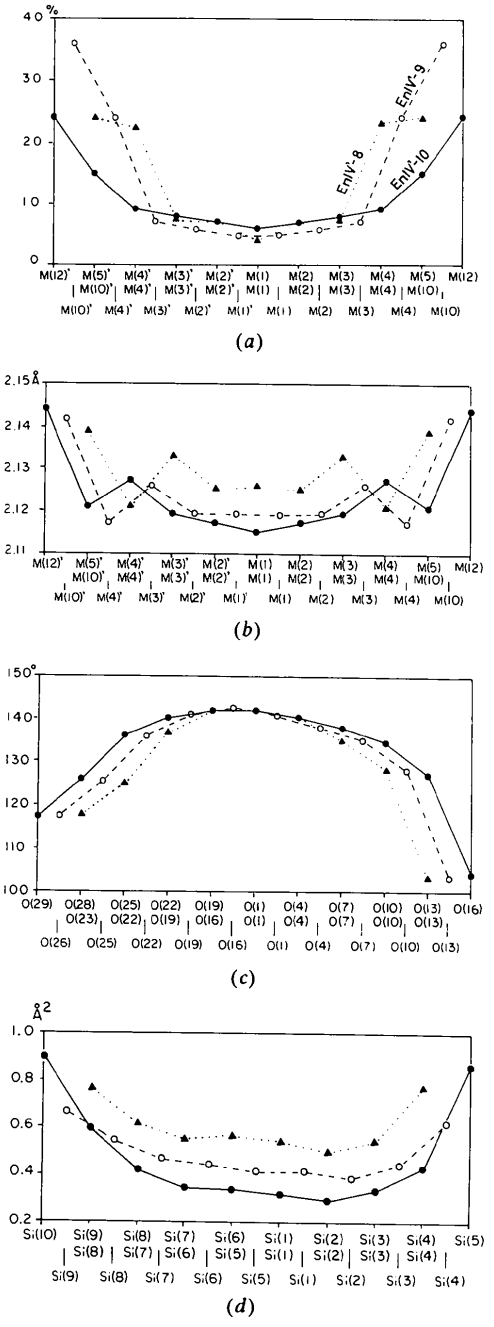

Fig. 1. (*a*) A plot of the Sc contents of the **M1** octahedra in the CPX slab. The octahedral sites are indicated, along the horizontal axis, successively from that at one end of the array of the octahedra through to that at the other end. The top of the three rows of symbols of the octahedral sites gives sites for EnIV'-10, the middle for EnIV'-8, and the bottom for EnIV'-9. The solid, broken, and dotted lines show the modes of variation in Sc content for EnIV'-10, EnIV'-9, and EnIV'-8, respectively. The symbols with primes represent the octahedral sites which are symmetrically related to those having the corresponding symbols without primes. Note that (*b*), (*c*) and (*d*) have been prepared as for (*a*). (*b*) A plot of mean bond lengths of individual **M1** octahedra. (*c*) A plot of Si–O–Si angles in the finite silicate chains. (*d*) A plot of the isotropic temperature factors of the Si atoms.

Table 8. *Atomic contents of the cation sites of the En*IV′ *structures*

Atomic site	Equipoint	Corresponding site in pyroxene	Contents Mg	Contents Sc
EnIV'-10				
M(1)	2(*e*)	*M*(1)	0·94(1)	0·06
M(2)	4(*g*)		0·93(1)	0·07
M(3)	4(*g*)		0·92(1)	0·08
M(4)	4(*g*)		0·91(1)	0·09
M(5)	4(*g*)		0·84(1)	0·15
M(12)	2(*b*)		0·76(1)	0·24
M(7)	2(*e*)	*M*(2)	0·98(1)	0·02
M(8)	4(*g*)		0·99(1)	0·01
M(9)	4(*g*)		0·99(1)	0·01
M(10)	4(*g*)		0·99(1)	0·01
M(11)	4(*g*)		0·95(1)	0·05
M(6)	4(*g*)		0·96(1)	0·00
T	2(*f*)		0·22 Si	0·04 Mg
EnIV'-9				
M(1)	8(*f*)	*M*(1)	0·94(1)	0·05
M(2)	8(*f*)		0·93(1)	0·06
M(3)	8(*f*)		0·93(1)	0·07
M(4)	8(*f*)		0·76(1)	0·24
M(10)	4(*b*)		0·64(1)	0·36
M(6)	8(*f*)	*M*(2)	0·98(1)	0·01
M(7)	8(*f*)		0·98(1)	0·01
M(8)	8(*f*)		0·98(1)	0·01
M(9)	8(*f*)		0·90(1)	0·10
M(5)	8(*f*)		0·98(1)	0·00
T	4(*e*)		0·12 Si	0·16 Mg
EnIV'-8				
M(1)	2(*e*)	*M*(1)	0·96(1)	0·04
M(2)	4(*g*)		0·93(1)	0·07
M(3)	4(*g*)		0·93(1)	0·07
M(4)	4(*g*)		0·77(1)	0·23
M(10)	2(*b*)		0·76(1)	0·24
M(6)	2(*e*)	*M*(2)	0·98(1)	0·02
M(7)	4(*g*)		0·98(1)	0·02
M(8)	4(*g*)		0·99(1)	0·01
M(9)	4(*g*)		0·90(1)	0·10
M(5)	4(*g*)		0·97(1)	0·03
T	2(*f*)		0·02 Si	0·30 Mg

compositions of EnIV′, however, show that the Sc contents per formula unit are close to three rather than four. Consequently, the following modification of (4) will better represent the chemical compositions of EnIV′:

$$[Mg_{(x-7\cdot5)/3}Sc_3][Mg_{2/3}Si_{(x-4)/3}]O_x \qquad (5)$$

with $x = 100$, 112, or 124. The expression of this

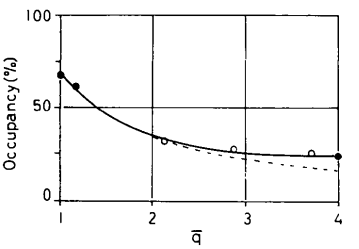

Fig. 2. A plot of atomic occupancy at the *T* site *versus* mean charge, $\bar{q}$, of the atoms located at *T*. The solid circles are for the crystals of En-IV (see part I) and open circles for those of EnIV′. The solid line defined by the entries is very close to the relation $N = 2/3\bar{q}$, as shown by the broken curve (N represents an occupancy).

Table 9. *Contents, mean charge, $\bar{q}$, and the number, n, of the cations at T, showing mean T–O distances,* $\overline{T\text{–O}}$

N	Sc/Mg	Contents	$\bar{q}$(e)	n*	$\overline{T\text{–O}}$ (Å)
En-IV-N series					
8	0·164	0·67 Li	1	1·34	1·999 (5)
10	0·08	0·58 Li 0·035 Si	1·17	1·23	2·00 (2)
9	0·118†	0·244 Si	4	0·49	2·00 (2)
EnIV′-N series					
8	0·088	0·30 Mg 0·02 Si	2·13	0·64	2·00 (1)
9	0·085	0·16 Mg 0·12 Si	2·86	0·56	2·00 (1)
10	0·065	0·04 Mg 0·22 Si	3·69	0·52	2·00 (1)

* Per formula unit: for 124, 112 and 100 O atoms for the En-IV-10, En-IV-9 and En-IV-8 types, respectively.
† Sc/(Mg + Co).

formula is an idealized version of the real compositions in the sense that the T site is assumed to be occupied only by Mg, no consideration being made of the possible location of Si at T.

It is notable that from a starting material containing a minor amount of Al_2O_3, a crystal was obtained having chemical composition: MgO 35·67, Sc_2O_3 7·94, SiO_2 53·17, and Al_2O_3 1·97wt % (analyst I. Steele). As the crystal has been found to have the structure type En-IV-8 by the X-ray precession method ($a = 9{\cdot}439$, $b = 8{\cdot}749$, $c = 21{\cdot}695$ Å, $\beta = 91°10'$), we may derive the structural formula from this composition in two ways:

$$(Mg_{29\cdot33}Sc_{4\cdot00})_{\Sigma=33\cdot33}[Mg_{1\cdot33}(Al_{1\cdot33}Si_{30\cdot60})]_{\Sigma=33\cdot33}O_{100},$$

and

$$(Mg_{30\cdot00}Sc_{4\cdot00})[Mg_{0\cdot66}(Al_{1\cdot33}Si_{30\cdot60})]O_{100}.$$

The first is almost exactly of the type of the ideal chemical formula for En-IV-8 (part I), while the second is closely similar to (4) with $x = 100$. In either case the Sc contents are higher compared to those of the above cases. Although the structural analysis of this crystal has not been carried out, it is very likely that the Al atoms in the structure would be located in the tetrahedra at the ends of the chain units; the resulting deficiency in the valence sums at the O atoms forming the tetrahedra about T would be balanced by higher contents of Sc in the polyhedra surrounding T than those of the present cases.

We may now conclude that the occupancy at T does not exceed $\frac{2}{3}$ in the En-IV structure types and the contents in the tetrahedra about T are sensibly adjusted so as to attain charge balance of the O atoms of the tetrahedra.

*Further structural complexity of En*IV′

Apparently single crystals of EnIV′ were sometimes found to be composites of different structure types. Thus, for example, the diffraction pattern of a crystal having the EnIV′-10 structure type was accompanied by that of an EnIV′-9 type in such a way that their reciprocal lattices are in parallel positions. Or, in another crystal, EnIV′-9 and EnIV′-8 coexisted. While examining crystals by the X-ray precession method, we encountered a crystal which was a composite of EnIV′-10 and EnIV′-9, the latter being dominant. A closer examination of the precession photograph, showing the $h0l$ reflections, revealed the existence of extra reflections in addition to those of the two structure types (Fig. 3). The reflections were not accounted for even if we assume new structures such as EnIV′-11, EnIV′-12 or others in the EnIV′-N series. It appears that the En-IV-N structure types are in fact limited to three for which $N = 8$, 9, and 10. The structural features of EnIV′ underlying the occurrence of these kinds of extra reflections will be discussed elsewhere.

Part of the crystal syntheses were carried out under the supervision of Professor O. J. Kleppa, Materials Research Laboratory of the University of Chicago, funded by the National Science Foundation; we are grateful to him for his encouragement. We also thank Dr Ian M. Steele for his electron-microprobe analyses, and Dr A. G. de L'Eprevier for his assistance

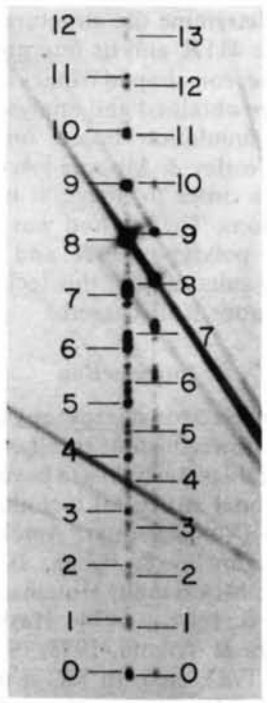

Fig. 3. Portion of the precession photograph (Cu K) of a composite crystal consisting of an EnIV′-10 structure and an EnIV′-9 structure, showing extra reflections in the composite $\bar{2}0l$ reciprocal-lattice row. The left of the pair of columns of figures gives the l indices of EnIV′-9 and the right those of EnIV′-10, those for EnIV′-9 being halved.

with the crystal synthesis. The structural study of EnIV′ was supported by Grant-in-Aid for Scientific Research 242016 of the Ministry of Education of Japan. Computations were carried out on a HITAC 8800/8700 computer at the Computer Centre of the University of Tokyo.

References

COPPENS, P. & HAMILTON, W. C. (1970). *Acta Cryst.* A**26**, 71–83.

HAWTHORNE, F. C. & GRUNDY, H. D. (1977). *Can. Mineral.* **15**, 50–58.

International Tables for X-ray Crystallography (1962). Vol. III, pp. 201–209. Birmingham: Kynoch Press.

SMYTH, J. R. & ITO, J. (1977). *Am. Mineral.* **62**, 1252–1257.

TAKÉUCHI, Y., KUDOH, Y. & ITO, J. (1977). *Proc. Jpn Acad.* **53**, 60–63.

TAKÉUCHI, Y., KUDOH, Y. & ITO, J. (1984). *Acta Cryst.* B**40**, 115–125.

WUENSCH, B. J. & PREWITT, C. T. (1965). *Z. Kristallogr.* **122**, 24–59.

Acta Cryst. (1984). B**40**, 132–138

High-Resolution Electron Microscopic Studies on a New Polytype of SiC and its Intergrowth Structures

BY R. S. RAI, P. KORGUL* AND G. SINGH

Department of Physics, Banaras Hindu University, Varanasi-221005, India

(*Received* 18 *April* 1983; *accepted* 12 *October* 1983)

Abstract

Tilted-beam two-dimensional lattice images have been used to determine the structure of a new polytype of SiC, *viz* 411*R*, and its intergrowth structures. Initially, the chevron-shaped fringes in a simple structure of 6*H* were obtained and analysed with the help of computer simulation based on the multislice approach of Cowley & Moodie [*Acta Cryst.* (1957), **10**, 609–619] in order to arrive at optimum experimental conditions. The method was then applied to a high-period polytype 411*R* and its intergrowth structures. The suitability of this technique for structural investigations is discussed.

Introduction

High-resolution electron microscopy (lattice imaging) has become a powerful tool to elucidate the details at ultrastructural level which are beyond the reach of more conventional structural techniques such as X-ray diffraction (Van Landuyt, Amelinckx, Kohn & Eckart, 1974; Cowley & Iijima, 1972; Allpress & Sanders, 1973; McConnell, Hutchison & Anderson, 1974; Buseck & Iijima, 1974; Hashimoto, Endoh, Takai, Tomioka & Yokota, 1978/79; Van Tendeloo & Amelinckx, 1982, *etc.*). In SiC it is usually found that large unit cells consist of regular stackings of unit cells of one or more common structure types like 6*H*, 15*R*, 4*H* and 21*R* (Verma & Krishna, 1966; Dubey, Ram & Singh, 1973). The utility of low-resolution lattice images has already been established in the structural investigations of SiC structures of large cell parameters (Dubey & Singh, 1978; Singh & Singh, 1980; Singh, Singh & Van Tendeloo, 1981; Yessik, Shinozaki & Sato, 1975; Ogbuji, Mitchell & Heuer, 1981; Kuo, Zhou, Ye & Kuo, 1982). It has been suggested by Jepps, Smith & Page (1979) that tilted-beam two-dimensional lattice images are capable of directly revealing the stacking sequence in SiC polytype structures. Recently, Smith & O'Keefe (1983) have very critically examined the conditions for obtaining direct structure images in small-period polytypes with the help of computer simulation using Optronics Photo-Write and HREM's from the 600 kV Cambridge microscope. Their computer simulations using a variety of experimental parameters leading to a resolution limit of 0·2 nm have shown that the tetrahedral stacking can be directly recognized under very restricted imaging conditions for crystal thicknesses up to about 7·5 nm.

Computer simulation of image contrast using the multislice approach (Cowley & Moodie, 1957; Goodman & Moodie, 1974) has generally been used for confirming the inferences from the lattice images. This requires advance knowledge of the structure as well as experimental parameters like foil thickness, defocus *etc.*, some of which are not easily found. In addition, the multislice computations become too cumbersome in cases of large polytype unit cells. Therefore, the use of computer simulation in this study has been confined to a well known structure of

* Crystallography Laboratory, The University of Newcastle upon Tyne, Newcastle upon Tyne, NE1 7RU, England.

0108-7681/84/020132-07$01.50